IJMSIT

International Journal of Multidisciplinary Studies and Innovative Technologies

Volume : 5
Number: 2
Year: 2021
Pages: 147 - 150

Synthetic Skin Cancer Image Data Generation Using Generative Adversarial Neural Network

Burak Beynek [1*], Şebnem Bora [2] Vedat Evren [3] and Aybars Uğur [4]

[1]*Department of Software Engineering/Faculty of Engineering, KIRKLARELI UNIVERSITY, Kirklareli, Turkey*
[2]*Department of Computer Engineering/Faculty of Engineering, EGE UNIVERSITY, İzmir, Turkey*
[3]*Department of Physiology, Basic Sciences/Faculty of Medicine, EGE UNIVERSITY, İzmir, Turkey*
[4]*Department of Computer Engineering/Faculty of Engineering, EGE UNIVERSITY, İzmir, Turkey*
[*]*Corresponding author: burakbeynek@klu.edu.tr*

Abstract – In this study, synthetic data generating method using generative adversarial neural network (GAN) for the skin cancer types malignant melanoma and basal-cell carcinoma is presented. GAN is a neural network where two synthetic networks compete. The generator attempts to generate data similar to those measured and the discriminator attempts to classify data as dummy or real. Using medical data in studies is a difficult task due to legal and ethical restrictions. Most of the available data is classified because of patient consent and available data in most cases is not labeled, low quality and/or low quantity. Recent GAN systems can generate labeled high quantity data without any personal discriminative information. In this paper, we used skin cancer images in The International Skin Imaging Collaboration (ISIC) database that have been used for discriminator training. To test our generated images applicability in the medical field studies we have conducted a Turing test with medical experts in various medical fields. Our results indicate that the generated data obtained with our method is a valuable alternative for real medical data.

Keywords – Deep Learning, Generative Adversarial Networks, Image generation, Medical Image Analysis, Skin Lesion

I. Introduction

The number of skin cancer patients in the world is continuously increasing and predicted to continue so [1]. Skin lesion type classifications also have a low accuracy rate. This is why diseases that can be treated nonsurgically cannot be prevented [2]. Reliable methods are needed in skin lesion diagnosis for clinical use. However, the data required to obtain such methods is not available.

Collecting data is no simple task especially in the medical field. There are some restrictions to collect medical data such as patient must give permission to share his data, legal and ethical requirements must be met to gain permissions, some diseases are so rare that sufficient amount of data cannot be collected, also there isn't a standard for collecting and storing the data, even if the data is collected most of the data is not labeled etc. Under these conditions collecting and using medical data is not an option in every medical field.

Generative models are implemented to create new data. Generative model is an unsupervised learning task that discovers and learns regularities or patterns in the input so that can generate new samples or output [3]. A remarkable progress has been achieved in recent years in generative models. In particular, many popular variants such as Generative Adversarial Network (GAN) [3], CycleGAN [4] and StarGAN [5] have emerged as a new standard to create various high-quality examples. The basic concept of GAN is the competition of the generator network and the discriminator network. The discriminator networks determines whether the given data is training data or not. The generator networks aims to deceive the discriminator by generating data similar to training data. The only input received by the generator during this period is the yes or no responses from the discriminator. The discriminator is trained with the training set. GANs were previously used in medical imaging [6]. Their fields of use include noise removal [7], image restoration [8], restoring image damages caused by metal implants [9], resolution enhancement [10], image synthesis [11], classification [12] and segmentation [13]. Despite giving promising results,

GANs have started being used in medicine just recently. To obtain usable anonymized medical data Togo et al. suggested a GAN method for generating synthetic gastritis images [14]. With loss function-based conditional progressive growing generative adversarial network (LC-PGGAN), they generated gastric X-ray images that had characteristics of gastritis/non-gastritis like real data. Han et al. suggested another GAN method for generating synthetic multi-sequence brain Magnetic Resonance (MR) [15]. Their GAN approach can generate 128x128 pixels brain MR slice images. They concluded that DCGAN model might be unsuitable for generating a whole 3D MR due to inferior realism and intensity. Schütte et al. proposed two GAN models for chest radiographs and brain computed tomography (CT) to generate anonymized images [16]. Both model's results were labeled by trained radiologists to determine the usability of generated images. As a result, %50 of the generated images were labeled as real.

The purpose of this study is to provide a minimal working example of a data reproduction tool for skin cancer image generation. There is no sufficient data available for use in skin cancer diagnosis and other related studies. Also, the use of data obtained from patients is limited due to ethical reasons. This study aims to eliminate the data shortage in this area. The validity of the obtained data can be tested using the Turing test.

The data can be used without requiring ethical permission as they are generated synthetically.

II. Materials and Method

A. Dataset

This study used the dataset collected by The International Skin Imaging Collaboration (ISIC) from 2016 to 2021 [17]. This dataset has a total of 70000 images in 10 types of skin cancers. Please refer to the ISIC official website for further information about the dataset. The images do not have a standard format or dimension. Some images are available as undiagnosed and unlabeled. The diseases malignant melanoma and basal-cell carcinoma have been selected for the study. 1000 images have been selected as training data for each disease from a total of 9100 images for these diseases. Features such as skin color, resolution, and image format have been taken into consideration in the selection process. Round-framed images taken with a microscope were eliminated to standardize the images. Also, images with digital or physical notes added on the skin or with unit lengths for measurement have been eliminated. (Figure I).

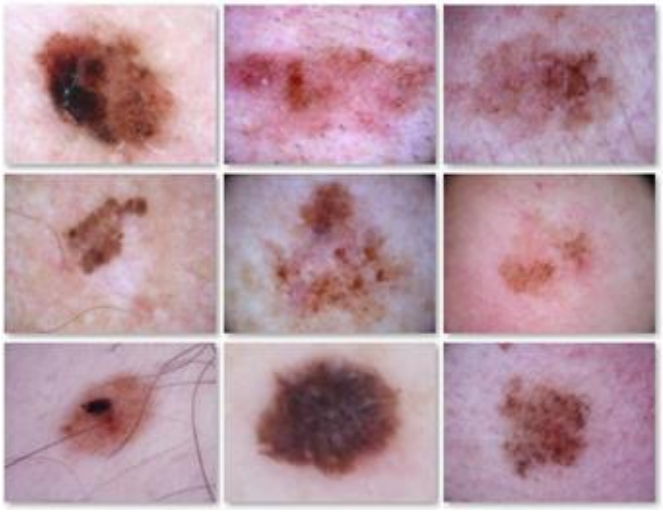

Figure I: Data Examples

B. Generative Adversarial Neural Network Architecture

The used GAN structure is an example of a deep convolutional GAN (DCGAN) [18]. The generator architecture used (Table I) consists of an input layer, four intermediary blocks, and an output layer. The last block has a convolution layer running on all the layers. The blocks use leakyReLU [19] as activation function and cross entropy as the loss function. The parameters 0.00015 learning ratio, $\beta 1 = 0.5$, $\beta 2 = 0.999$ and $\varepsilon = 1e\text{-}7$ and Adam-optimizer [20] were used in both the generator and the discriminator.

The discriminator architecture (Table II) is comprised of four blocks containing 2-dimensional convolution and 0.25 dropout [21] and an output block containing leveling and output layers. The convolutional layers use leakyReLU as activation function and cross entropy as the loss function.

Table 1. Generator Network Architecture

Layer (type)	Output Shape	Param
dense (Dense)	(None, 4096)	413696
reshape (Reshape)	(None, 4, 4, 256)	0
up_sampling2d (UpSampling2D)	(None, 8, 8, 256)	0
conv2d (Conv2D)	(None, 8, 8, 256)	590080
batch_normalization (BatchNormalization)	(None, 8, 8, 256)	1024
activation (Activation)	(None, 8, 8, 256)	0
up_sampling2d_1 (UpSampling2D)	(None, 16, 16, 256)	0
conv2d_1 (Conv2D)	(None, 16, 16, 256)	590080
batch_normalization_1 (BatchNormalization)	(None, 16, 16, 256)	1024
activation_1 (Activation)	(None, 16, 16, 256)	0
up_sampling2d_2 (UpSampling2D)	(None, 32, 32, 256)	0
conv2d_2 (Conv2D)	(None, 32, 32, 128)	295040
batch_normalization_2 (BatchNormalization)	(None, 32, 32, 128)	512
activation_2 (Activation)	(None, 32, 32, 128)	0
up_sampling2d_3 (UpSampling2D)	(None, 128, 128, 128)	0
conv2d_3 (Conv2D)	(None, 128, 128, 128)	147584
batch_normalization_3 (BatchNormalization)	(None, 128, 128, 128)	512
activation_3 (Activation)	(None, 128, 128, 128)	0
conv2d_4 (Conv2D)	(None, 128, 128, 3)	3459
activation_4 (Activation)	(None, 128, 128, 3)	0

Table 2. Generator Network Architecture

Layer (type)	Output Shape	Param
conv2d_5 (Conv2D)	(None, 64, 64, 32)	896
leaky_re_lu (LeakyReLU)	(None, 64, 64, 32)	0
dropout (Dropout)	(None, 64, 64, 32)	0
conv2d_6 (Conv2D)	(None, 32, 32, 64)	18496
zero_padding2d (ZeroPadding2D)	(None, 33, 33, 64)	0
batch_normalization_4 (BatchNormalization)	(None, 33, 33, 64)	256
leaky_re_lu_1 (LeakyReLU)	(None, 33, 33, 64)	0
dropout_1 (Dropout)	(None, 33, 33, 64)	0
conv2d_7 (Conv2D)	(None, 17, 17, 128)	73856
batch_normalization_5 (BatchNormalization)	(None, 17, 17, 128)	512
leaky_re_lu_2 (LeakyReLU)	(None, 17, 17, 128)	0
dropout_2 (Dropout)	(None, 17, 17, 128)	0
conv2d_8 (Conv2D)	(None, 17, 17, 256)	295168
batch_normalization_6 (BatchNormalization)	(None, 17, 17, 256)	1024
leaky_re_lu_3 (LeakyReLU)	(None, 17, 17, 256)	0
dropout_3 (Dropout)	(None, 17, 17, 256)	0
conv2d_9 (Conv2D)	(None, 17, 17, 512)	1180160
batch_normalization_7 (BatchNormalization)	(None, 17, 17, 512)	2048
leaky_re_lu_4 (LeakyReLU)	(None, 17, 17, 512)	0
dropout_4 (Dropout)	(None, 17, 17, 512)	0
flatten (Flatten)	(None, 147968)	0
dense_1 (Dense)	(None, 1)	147969

III. Results

The images to be generated were set to have the dimension of 128x128. Figure II shows the epoch/loss graphs for the generator and discriminator in the training conducted with 2000 iterations for malignant melanoma. As a result of the training, the generator loss value was found to be 9.2 and the discriminator loss value to be 0.09. The dummy images obtained from the training are shown in Figure III.

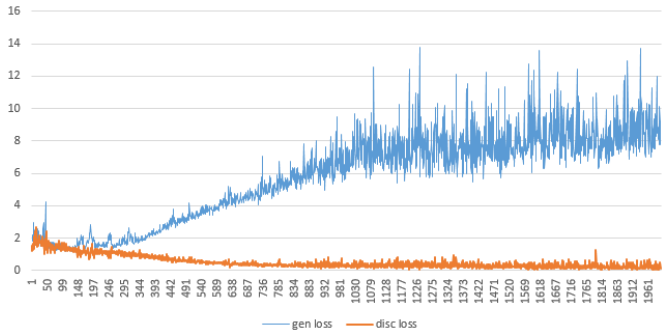

Fig. II Loss/ Epoch Graph for Malignant Melanoma

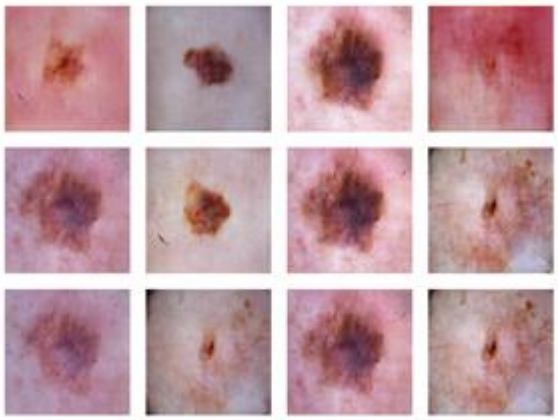

Fig. III Generated Examples of Malignant Melanoma

Figure IV shows the epoch/loss graphs for the generator and discriminator in the training conducted with 2000 iterations for basal-cell carcinoma. As a result of the training, the generator loss value was found to be 6.7 and the discriminator loss value to be 0.1. The dummy images obtained from the training are shown in Figure V.

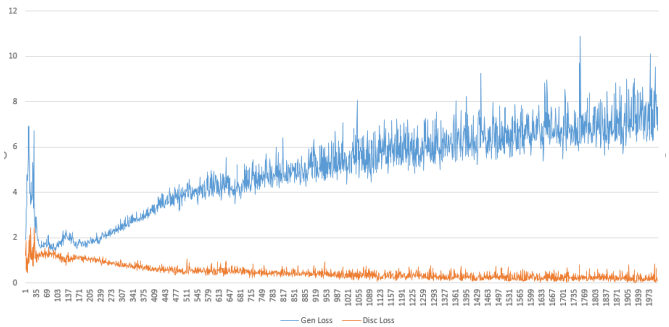

Fig. IV Loss/ Epoch Graph for Basal-Cell Carcinoma

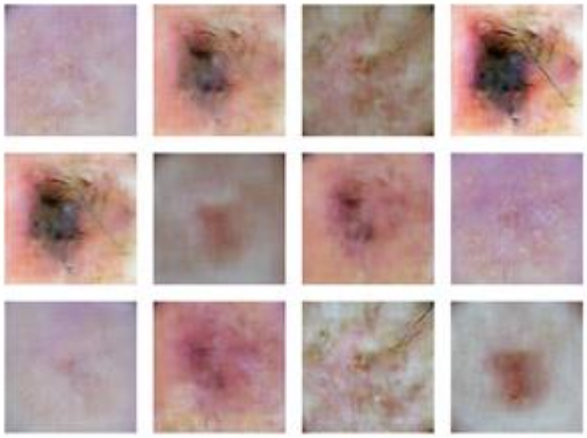

Fig. V Generated Examples of Basal-Cell Carcinoma

The malignant melanoma and basal-cell carcinoma images we obtained are shown side by side with original images in Figure VI and Figure VII. Comparing the images, it can be said that images similar to the original ones were generated. To confirm our findings, we applied a simple Turing test [22] to 65 medical professionals. In this test, we used 50 randomly sampled real and generated images for both malignant melanoma and basal cell carcinoma. Participants were told to label images as real or generated with an online form. Test results showed us avg. %58.72 of generated data has considered real.

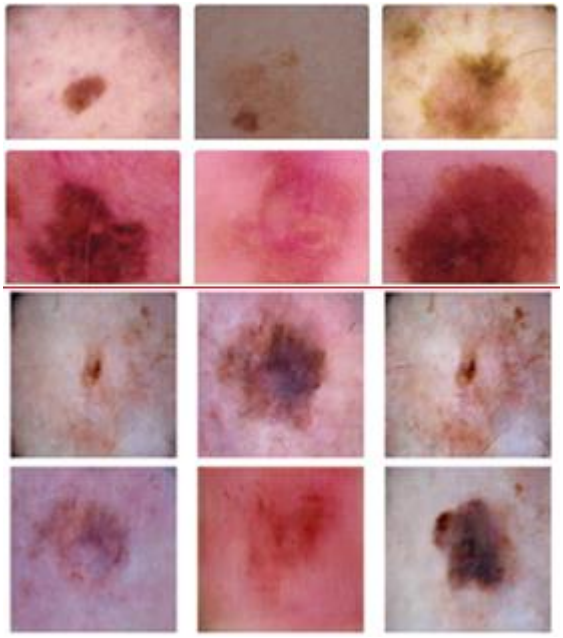

Fig. VI Original Images (Top), Generated Images (Bot.) of Malignant Melanoma

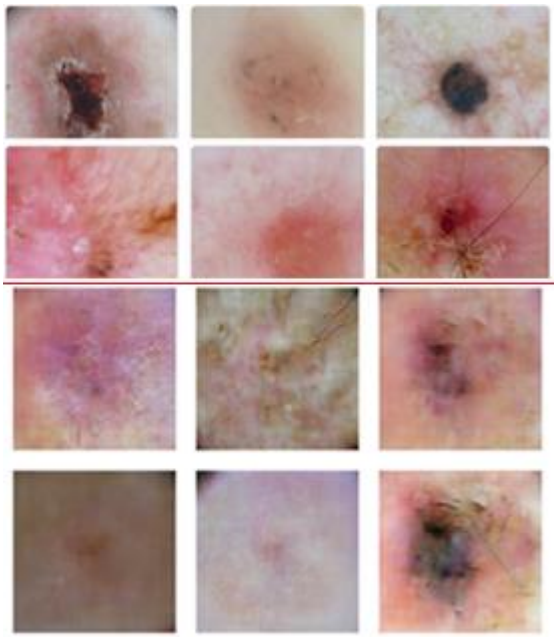

Fig. VII Original Images (Top), Generated Images (Bot) of Basal-Cell Carcinoma

IV. DISCUSSION

This study supports that the GAN models can generate valuable medical images. Unlike most of the previous studies this study confirmed this suggestion with a Turing test. %58.72 success rate shows us that the generated images are plausible but needs improvement. 128x128 generated image resolution is enough for human discrimination tests but may not be sufficient for every application and can be improved in future studies.

The fact that the images needed in medical studies could not be accessed for legal restrictions led us to find an alternative way. Our method solves this problem by generating anonymous medical images. The generated data can be used in artificial intelligence methods to identify and classify diseases such as basal-cell carcinoma for which few samples are available. This will enable designing artificial intelligence systems for diseases on which studies cannot be conducted due to insufficient data.

V. CONCLUSION

We have proposed a synthetic skin cancer image data generation method with generative adversarial networks, which is an anonymous medical image generation method for supplying future artificial intelligence studies with labeled data. In the light of the Turing tests results we can say that the proposed model can generate convenient medical images for skin cancer medical research applications.

ACKNOWLEDGMENT

The authors would like to thank all medical professionals for participating in the Turing test for this study.

REFERENCES

[1] B. Møller, H. Weedon-Fekjær, T. Hakulinen, L. Tryggvadottir, H. Storm, M. Talb¨ack, and T. Haldorsen, “Prediction of cancer incidence in the Nordic countries up to the year 2020,” European journal of cancer prevention: the official journal of the European Cancer Prevention Organization (ECP), vol. 11 Suppl 1, pp. S1–96, 2002.

[2] C. F. Heal, B. A. Raasch, P. Buettner, and D. Weedon, “Accuracy of clinical diagnosis of skin lesions,” British Journal of Dermatology, vol. 159, no. 3, pp. 661–668, 2008.

[3] I. J. Goodfellow, J. Pouget-Abadie, M. Mirza, B. Xu, D. Warde Farley, S. Ozair, A. Courville, and Y. Bengio, “Generative adversarial networks,” arXiv preprint arXiv: 1406.2661, 2014.

[4] J.. Zhu, T. Park, P. Isola, and A. A. Efros. “Unpaired image-to-image translation using cycle-consistent adversarial networks,” in Proceedings of the IEEE international conference on computer vision, pages 2223–2232, 2017.

[5] Y. Choi, M. Choi, M. Kim, J. Ha, S. Kim, and J. Choo. “Stargan: Unified generative adversarial networks for multi-domain image-to-image translation,” in Proceedings of the IEEE Conference on Computer Vision and Pattern Recognition, pages 8789–8797, 2018.

[6] X. Yi, E. Walia, and P. Babyn, “Generative adversarial network in medical imaging: A review,” Medical Image Analysis, vol. 58, p. 101552, 2019.

[7] J. M. Wolterink, T. Leiner, M. A. Viergever, and I. I˙sgum, “Generative adversarial networks for noise reduction in low-dose CT,” IEEE transactions on medical imaging, vol. 36, no. 12, pp. 2536–2545, 2017.

[8] S. U. H. Dar, M. Yurt, M. Shahdloo, M. E. Ildız, and T. C¸ Ukur, “Synergistic reconstruction and synthesis via generative adversarial networks for accelerated multi-contrast mri,” arXiv preprint arXiv: 1805.10704, 2018.

[9] J. Wang, Y. Zhao, J. H. Noble, and B. M. Dawant, “Conditional Generative Adversarial Networks for Metal Artifact Reduction in CT Images of the Ear,” in International Conference on Medical Image Computing and Computer-Assisted Intervention. Springer vol 11070, pp. 3–11, 2018.

[10] C. You, G. Li, Y. Zhang, X. Zhang, H. Shan, M. Li, S. Ju, Z. Zhao, Z. Zhang, W. Cong, “CT super-resolution GAN constrained by the identical, residual, and cycle learning ensemble (GANCIRCLE),” IEEE Transactions on Medical Imaging, vol. 39, no. 1, pp. 188–203, 2019.

[11] M. J. Chuquicusma, S. Hussein, J. Burt, and U. Bagci, “How to fool radiologists with generative adversarial networks? a visual Turing test for lung cancer diagnosis,” in 2018 IEEE 15th international symposium on biomedical imaging (ISBI 2018), pp. 240–244, 2018.

[12] X. Yi, E. Walia, and P. Babyn, “Unsupervised and semi-supervised learning with Categorical Generative Adversarial Networks assisted by Wasserstein distance for dermoscopy image Classification,” arXiv preprint, arXiv: 1804.03700, 2018.

[13] Z. Zhang, L. Yang, and Y. Zheng, “Translating and segmenting multimodal medical volumes with cycle-and shape-consistency generative adversarial network,” 2018 IEEE/CVF Conference on Computer Vision and Pattern Recognition, 9242-9251, 2018.

[14] R. Togo, T. Ogawa and M. Haseyama, "Synthetic Gastritis Image Generation via Loss Function-Based Conditional PGGAN," in IEEE Access, vol. 7, pp. 87448-87457, 2019.

[15] C. Han, H. Hayashi, L. Rundo, R. Araki, W. Shimoda, S. Muramatsu, Y. Furukawa, G. Mauri, H. Nakayama, "GAN-based synthetic brain MR image generation," 2018 IEEE 15th International Symposium on Biomedical Imaging, pp. 734-738, 2018.

[16] D. Schütte, A., Hetzel, J., Gatidis, S., “Overcoming barriers to data sharing with medical image generation: a comprehensive evaluation.”, NPJ, Digit. Med. 4, 141, 2021.

[17] (2021) International Skin Imaging Collaboration Website. [Online] Available: http://www.isdis.net/index.php/isic-project

[18] A. Radford, L. Metz, and S. Chintala, “Unsupervised Representation Learning with Deep Convolutional Generative Adversarial Networks,” arXiv preprint, arXiv: 1511.06434, 2016.

[19] A. L. Maas, A. Y. Hannun, and A. Y. Ng, “Rectifier nonlinearities improve neural network acoustic models,” in Proc. ICML, vol. 30, p. 3, 2013.

[20] D. P. Kingma and J. Ba, “Adam: A method for stochastic optimization,” arXiv preprint, arXiv: 1412.6980, 2014.

[21] N. Srivastava, G. Hinton, A. Krizhevsky, I. Sutskever, and R. Salakhutdinov, “Dropout: A Simple Way to Prevent Neural Networks from Overfitting,” Journal of Machine Learning Research, vol. 15, pp. 1929–1958, 2014.

[22] A. M. Turıng, “I.-Computıng Machınery and Intellıgence,” Mind, Volume LIX, Issue 236, pp. 433–460, 1950.